Powerful low-molecular-weight gelators based on L-valine and L-isoleucine with various terminal groups

Masahiro Suzuki,*[a] Teruaki Sato,[b] Hirofusa Shirai[b] and Kenji Hanabusa[a]

Received (in Montpellier, France) 4th April 2006, Accepted 16th May 2006
First published as an Advance Article on the web 5th June 2006
DOI: 10.1039/b604847a

Novel L-valine and L-isoleucine gelators, which have various terminal groups, such as an ester, carboxylic acid and carboxylate as well as different alkyl chain lengths between the terminal group and L-amino acid segment, were synthesized and their organogelation properties were examined in various organic solvents and oils. The organogelation properties significantly depended on the molecular structures of the L-amino acid, the length of the alkyl chains and hydrophilic–hydrophobic balance of the gelators. The FT-IR studies demonstrated that the driving forces for the organogel formation were the hydrogen bonding and van der Waals interactions, and the aggregation modes of the nanofibers depended on the solvents. Furthermore, it was found that these gelators were useful for the selective gelation of oils or fuels from oil/water mixtures.

Introduction

Low-molecular-weight gelators, which form organogels (organogelators) and hydrogels (hydrogelators), have been significantly investigated because of not only their academic interest, but also because of their potential wide applications in industrial fields, such as cosmetics, foods, medical science and tissue engineering.[1–4] Such gelators, which are small molecules, form various supramolecular polymers, such as fibers, ribbons and sheets through hydrogen bonding, van der Waals (hydrophobic) and π-stacking interactions, and create a three-dimensional network, leading to the formation of supramolecular gels. Recently, the nanostructures formed by gelators (in addition to their gelation properties) have received increased attention and have been used as organic templates for the fabrication of mesoporous polymers and nanostructured inorganic materials.[5,6] The sol–gel polymerization of various metal alkoxides (Si, Ti, Ta, V, *etc.*) in organogels produces various nanostructured metal oxides, such as helical nanofibers, nanotubes, nanoribbons and nanoparticles.[6]

We have developed good gelators that are simply and effectively synthesized and environmentally friendly materials (having features such as biodegradation and/or no toxicity). L-Amino acid-based gelators are some of the best gelators according to the following concepts: L-amino acids are safe for the environment and living organisms, most L-amino acids are commercially available (as relatively cheap starting materials), and the synthetic methodologies for many amino acid-based compounds are already established. In this paper, we describe the synthesis of novel low-molecular-weight gelators based on L-valine and L-isoleucine and their gelation properties.

Results and discussion

Syntheses

These compounds were prepared according to the procedure illustrated in Scheme 1. The ester compounds were prepared by acylation of L-valylaminooctadecane or L-isoleucylamino-octadecane[7] with diacid chloride monoalkyl esters with high yields (>90%). Deesterification in an aqueous THF solution containing NaOH led to the carboxylic acid compounds being obtained. The neutralization of the carboxylic acids then leads to the formation of the sodium salts. The synthetic procedures involve a multi-step organic synthesis, and are not easier than those of the salt-type gelators.[3g] However, each process is simple and these organogelators are obtained in relatively high reaction yields.

Organogelation properties

Although some evaluation methods for gelation have been reported,[2b] we evaluated the organogelation using a test tube inversion method. The organogelation properties of all compounds at 25 °C are listed in Table 1. Here, these values denote the minimum gel concentration (MGC, g L^{-1}) of gelators necessary for gelation. The ester compounds based on L-valine (**1a**, **4a**, **7a**) have good organogelation ability and form organogels in many organic solvents, such as alkanes, alcohols, esters, ketones, cyclic ethers, aromatic solvents, polar solvents, oils and silicon oils. Especially, **7a** also forms an organogel in chloroform, and is a powerful gelator. The L-isoleucine esters (**1b**, **4b**, **7b**) also show a good organogelation behaviour. A dependence of the organogelation abilities on the alkyl chain length between the ester group and L-isoleucine segment was observed; **4b** had a better organogelation ability than **1b** and **7b**; **1b** does not gel alcohols, while **7b** does not gel polar solvents, such as alcohols, DMF and DMSO. In addition, the gelation ability of **4b** is comparable to **4a**, while those of **1b** and **7b** are less powerful than the corresponding **1a** and

---

[a] *Graduate School of Science and Technology, Shinshu University, Ueda, Nagano 386-8567, Japan. E-mail: msuzuki@giptc.shinshu-u.ac.jp; Fax: +81 268 21 5608; Tel: +81 268 21 5415*
[b] *Department of Functional Polymer Science, Faculty of Textile Science and Technology, Shinshu University, Ueda, Nagano, 386-8567, Japan*

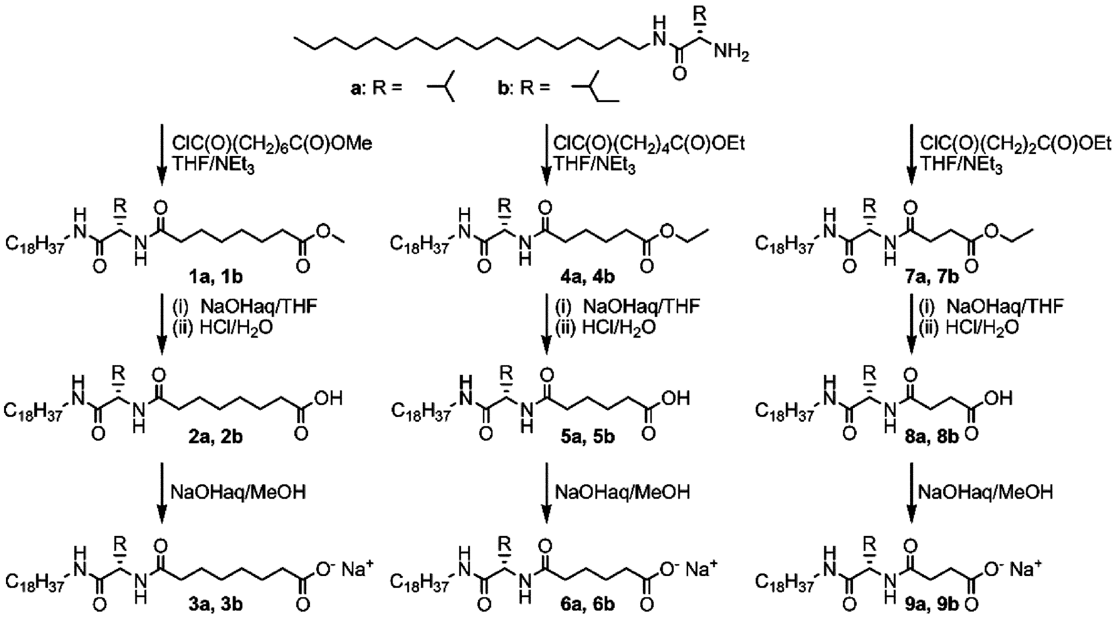

Scheme 1 Synthetic procedure for organogelators.

7a. These results indicate that a hydrophilicity–hydrophobicity balance, which should be sensitively reflected by the slightly changing alkyl chain lengths and molecular structures (amino acid segment), is very important for the organogelation, and **7a** and **4b**, having a suitable balance function, act as powerful organogelators.

Among the carboxy-type gelators (**2a**, **5a**, **8a**), **8a** showed the best organogelation behaviour, which was similar to the ester-

Table 1 Gelation properties of **1**–**9** at 25 °C[a]

	L-Valine derivatives									L-Isoleucine derivatives								
	Ester			Carboxylic acid			Na salt			Ester			Carboxylic acid			Na salt		
Solvent	**1a**	**4a**	**7a**	**2a**	**5a**	**8a**	**3a**	**6a**	**9a**	**1b**	**4b**	**7b**	**2b**	**5b**	**8b**	**3b**	**6b**	**9b**
n-Hexane	3	2	8	7	—	30	In	In	In	5	4	16	7	In	—	In	In	In
n-Dodecane	16	4	4	10	4	4	—	8	—	—	4	3	—	10	20	20	40	—
Cyclohexane	20	3	8	12	20	In	In	In	In	7	6	8	1	6	—	—	In	40
MeOH	8	7	14	20	20	20	—	—	—	—	13	—	12	18	—	35	20	—
EtOH	15	12	14	25	40	30	50	50	20	—	13	—	15	20	30	18	40	20
^{1}PrOH	30	38	20	—	40	—	40	50	10	—	20	—	25	40	—	15	40	20
AcOEt	5	6	8	—	—	20	In	In	In	4	8	30	5	16	—	In	In	In
Acetone	5	4	6	8	—	20	In	In	In	7	6	20	5	20	—	In	In	In
THF	—	40	40	—	—	—	—	In	20	—	—	—	30	—	—	In	20	30
1,4-Dioxane	12	10	14	—	15	20	In	In	I	10	10	16	8	25	20	In	In	In
$PhCH_3$	10	8	20	25	15	8	—	—	—	14	10	16	3	12	6	—	40	—
PhCl	17	10	20	30	15	20	—	50	—	17	13	12	5	12	12	15	20	40
$PhNO_2$	4	3	8	12	—	10	—	—	20	5	4	30	3	12	—	5	—	10
DMF	7	8	20	30	40	30	—	—	10	7	6	—	12	16	20	10	40	10
DMSO	7	5	8	20	40	40	—	40	10	3	4	—	3	14	6	15	40	10
$CHCl_3$	—	—	20	—	—	30	—	50	40	—	—	—		—	30	—	—	40
CH_3CN	3	4	14	—	—	20	In	In	In	5	4	20	0.7	24	In	In	—	In
Salad oil	10	10	8	10	5	8	20	40	5	8	3	8	10	7	20	35	5	5
Silicone oil	10	4	3	—	—	13	—	—	—	15	4	8	—	In	40	35	—	40
Linseed oil	15	8	8	10	4	13	20	40	10	8	8	12	10	7	30	40	4	10
Si4	20	10	14	—	In	In	In	In	In	18	6	12	—	—	—	In	In	In
Si5	20	8	6	—	In	In	In	In	In	15	6	6	—	—	—	In	In	In
IPM	15	5	6	5	5	13	10	30	—	12	4	12	30	18	—	40	5	30
Paraffin	12	5	3	10	5	4	30	5	40	12	10	8	12	16	16	10	5	40
Triolein	12	7	14	10	7	8	15	13	20	12	8	12	12	10	6	8	7	5
Kerosene	30	8	3	30	20	13	30	20	—	13	4	8	10	12	20	30	20	—
PC	5	4	8	30	5	10	30	8	In	6	4	16	5	20	—	10	10	In

[a] Values denote minimum gel concentration (MGC, g L^{-1}). In: Almost insoluble. —: No gelation at 40 g L^{-1}. Si4: Octamethylcyclotetrasiloxane. Si5: Decamethylcyclopentasiloxane. IPM: Myristic acid isopropyl ester. PC: Propylene carbonate.

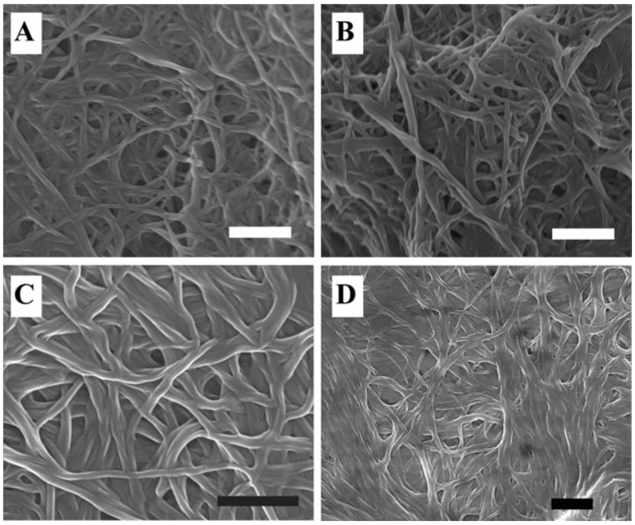

Fig. 1 FE-SEM images of dried gels prepared from toluene gels based on **1a** (A) and **1b** (B) as well as ethanol gels based on **3b** (C) and **9b** (D): [**1a**] = 10 mg mL^{-1}, [**1b**] = 15 mg mL^{-1}, [**3b**] = [**9b**] = 20 mg mL^{-1}. Scale bars are 200 nm.

type gelators. However, the organogelation abilities generally decreased compared to the ester-type gelators. This should be attributed to the change in the hydrophilic–hydrophobic balance by deesterification and the intermolecular interactions by the carboxy group. In contrast, **2b** gelled almost the same solvents as **5b**, whereas **2b** had smaller MGC values (better gelation abilities) than **5b**. Compared with **1b**, **2b** forms organogels in alcohols and THF. The organogelation abilities of **8b** are lower than those of **7b**.

For the sodium salt-type gelators, the solubility in organic solvents decreased and the gelators were insoluble in *n*-hexane, ethyl acetate, acetone, dioxane and cyclic silicone solvents. As these gelators possess a charge, they have a more hydrophilic feature, therefore, leading to their low solubility and decrease in gelation ability. The organogelation abilities for the L-valine derivatives significantly depend on the length of the alkyl chains between the amino acid segment and charged group. **9a**, possessing short alkyl chains, shows a relatively good organogelation ability compared to the other charged gelators. In contrast, the charged gelators of L-isoleucine show similar organogelation abilities (no dependence on the alkyl chain length). In addition, because these sodium salt-type compounds are water-soluble (but do not function as a hydrogelator), they are water-soluble organogelators.

FE-SEM observation

It is well-known that a supramolecular gel is often formed by self-assembled nanofibers.[2,3] Such superstructures consisting of the gelators in organogels were observed using field emission scanning electron microscopy. Fig. 1 shows the FE-SEM images of dried gels prepared from toluene gels based on **1a** and **1b** as well as ethanol gels based on **3b** and **9b**. Here, **1a** and **1b** form a transparent toluene gel, and **9b** forms an opaque ethanol gel. In the transparent toluene gels, **1a** and **1b** created a three-dimensional network formed by the entanglement of self-assembled nanofibers with a diameter of several tens of nanometers. In contrast, the self-assembled nanofibers formed by **3b** and **9b** are several hundred of nanometers long. The large size nenofibers lead to the formation of the opaque ethanol gel. The organogels are formed by entrapping solvent molecules into the nanospaces of the three-dimensional network.

FT-IR study

Supramolecular polymers in organogels are often formed through non-covalent interactions, such as hydrogen bonding and van der Waals forces. IR spectroscopy is a powerful tool for studying these interactions, thus we measured the FT-IR spectra. Fig. 2 shows the FT-IR spectra of **2b** in chloroform solution and DMSO gel. In a chloroform solution that most gelators can not gel, the typical absorption bands, characteristic of the non-hydrogen bonded amide groups, were observed around 3433 cm^{-1} (νN–H), 1657 cm^{-1} (νC=O) and 1509 cm^{-1} (δN–H). In contrast, the IR peaks of the DMSO gel appeared around 3290 cm^{-1} (νN–H), 1635 cm^{-1} (νC=O) and 1560 cm^{-1} as well at 1540 cm^{-1} (δN–H) due to hydrogen bonded amide groups. This result indicates that one of the driving forces for organogelation is the intermolecular hydrogen bonding between the amide groups. In addition, the absorption bands arising from the antisymmetric (ν_{as}C–H) and symmetric (ν_sC–H) stretching vibrations of the alkyl chains were observed at 2929 cm^{-1} and 2856 cm^{-1} in chloroform solution, indicating the presence of a *gauche* form alkyl chain. These IR bands appeared at 2912 cm^{-1} (ν_{as}C–H) and 2850 cm^{-1} (ν_sC–H) in the DMSO gel, corresponding to the alkyl chain of the all-*trans* form. Such lower wavelength shifts of the IR bands of ν_{as}C–H and ν_sC–H demonstrate the decreased mobility of the alkyl chain; consequently, it is clear that the van der Waals interaction between the alkyl chains is present in the DMSO gel. On the other hand, the IR bands of

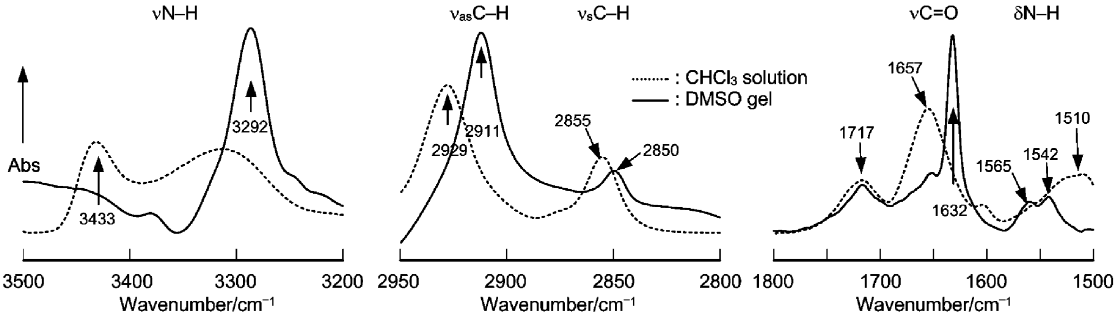

Fig. 2 FT-IR spectra of **2b** in chloroform solution (dashed line) and DMSO gel (solid line): [**2b**] = 10 g L^{-1}.

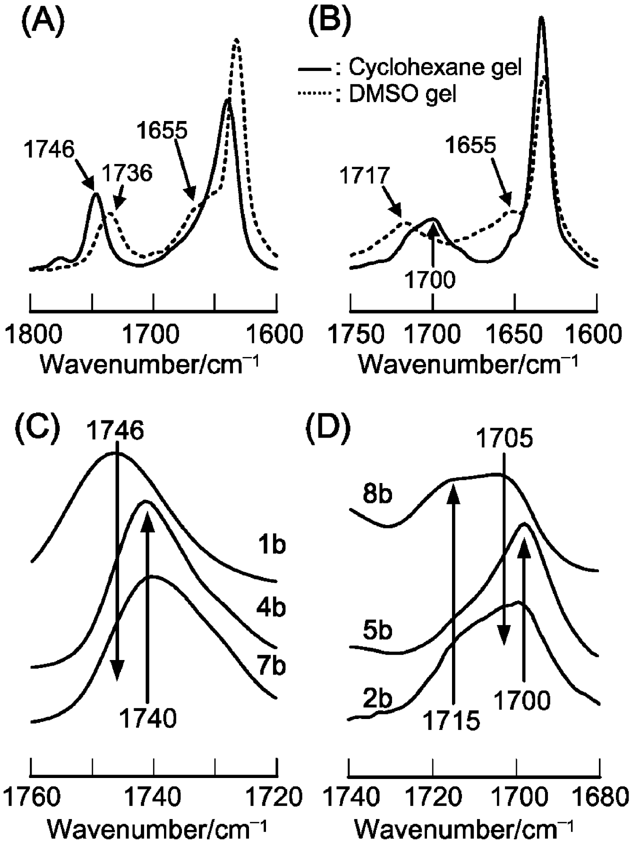

Fig. 3 FT-IR spectra of organogels: (A) cyclohexane gel (solid line) and DMSO gel (dashed line) based on **1b** (10 g L^{-1}); (B) cyclohexane gel (solid line) and DMSO gel (dashed line) based on **2b** (10 g L^{-1}); (C) cyclohexane gels based on **1b**, **4b** and **7b**; (D) cyclohexane gel based on **2b** (5 g L^{-1}) and dodecane gels based on **5b** (10 g L^{-1}) and **8b** (20 g L^{-1}).

the carboxy group are observed at 1717 cm^{-1} in the chloroform and DMSO gel, indicating that the carboxy group does not play an important role in the self-assembly in the DMSO gel.

Moreover, the FT-IR spectra of organogels of not only the polar solvent (DMSO), but also apolar solvents were measured. Fig. 3 shows the FT-IR spectra of various organogels and the IR data are listed in Table 2. For all the organogels, the IR bands, arising from the hydrogen-bonded amide groups, are independent of the solvents and appear around 3290 cm^{-1} (νN–H), 1635 cm^{-1} (νC=O, amide I) as well at 1560 and 1540 cm^{-1} (δN–H). These values were approximately consistent with those of the solid states. The hydrogen-bonding interaction between the amide groups is a key driving force for a one-dimensional self-assembly of gelators, and then it grows into a three-dimensional network by the entanglement of the nanofibers. As hydrogen bonding occurs in the core of the self-assembled nanofibers, it is probably hardly exposed to the solvents.

Table 2 FT-IR data for **1b**–**3b**

	νN–H	νC=O^a	Amide I	Amide II
1b				
$CHCl_3$	3433	1730	1657	1509
Cyclohexane gel	3292	1746	1640	1553
DMSO gel	3285	1736	1660, 1632	1561, 1544
Solid state^b	3290	1736	1635	1561
2b				
$CHCl_3$	3432	1717	1655	1510
Cyclohexane gel	3286	1699	1633	1558, 1543
DMSO gel	3286	1717	1652, 1632	1560, 1542
Solid state^b	3289	1710	1635	1561, 1544
3b				
DMSO gel	3290	—	1635, 1654	1565, 1540
Dodecane gel	3287	—	1635	1563, 1540
Solid state^b	3289		1636	1559, 1543

^{a} Ester group for **1b** and carboxy group for **2b**. ^{b} KBr pellet.

However, the IR bands of the non-hydrogen bonded amide group in addition to the hydrogen bonded one were observed around 1655 cm^{-1} in the DMSO gels, but did not appear in the cyclohexane or dodecane gels (Fig. 3(A) and (B)). In addition, the IR bands for the C=O stretching vibration of the ester and carboxy groups are changed by the solvents. For **1b**, the IR bands of νC=O (ester) appear at 1730 cm^{-1} in the chloroform solution, at 1736 cm^{-1} in the DMSO gel and solid state and at 1746 cm^{-1} in the cyclohexane gel. Considering little participation of the ester group in the self-assembly,[8] it is likely that the ester group is situated in aggregates thickly packed by the alkyl groups. For **2b**, the IR bands observed at 1700–1720 cm^{-1} arise from the carboxylic acid dimer;[9] *i.e.*, at 1717 cm^{-1} in the DMSO gel and chloroform solution and at 1699 cm^{-1} in the cyclohexane gel. It is noteworthy that the IR band in the DMSO gel is the same as that of the chloroform solution, which indicates that the interaction may be play a only slight role in the self-assembly into nanofibers in the DMSO gel. In contrast, the carboxy groups have a strong hydrogen-bonding interaction in the cyclohexane gel; they probably form a cyclic dimer. These IR results would indicate that the gelators form nanofibers with a different aggregation mode in polar and non-polar solvents.

The IR bands of the ester and carboxy groups also depend on the length of the alkyl chains; the ester νC=O bands are observed at 1740 cm^{-1} for **4b** and **7b** (Fig. 3(C)), and the carboxy νC=O bands are observed at 1700 cm^{-1} for **5b** and at 1705 cm^{-1} and 1715 cm^{-1} for **8b** (Fig. 3(D)). For the esters, the IR spectra of **4b** and **7b** in the cyclohexane gels are similar to those of their solid state spectra, indicating that they form nanofibers with a similar aggregation mode. On the other hand, **8b**, which has a short alkyl spacer (C2), shows two IR peaks in the dodecane gel, arising from the hydrogen bonded carboxy group, while one IR peak appeared at 1718 cm^{-1} in the solid state. It is likely that **8b** self-assembles into nanofibers through at least two hydrogen bonding modes.

Gelation mechanism and aggregation modes

The results of the IR studies allow us propose an organogelation mechanism as illustrated in Scheme 2. In the cyclohexane gel, the ester-type gelators self-assemble into one-dimensional nanofibers through a hydrogen bonding interaction, and their entanglement by a van der Waals interaction leads to the formation of a three-dimensional network (Scheme 2(A)). The carboxy-type gelators form a dimer through hydrogen bonding between the carboxy groups, and then the nanofibers are

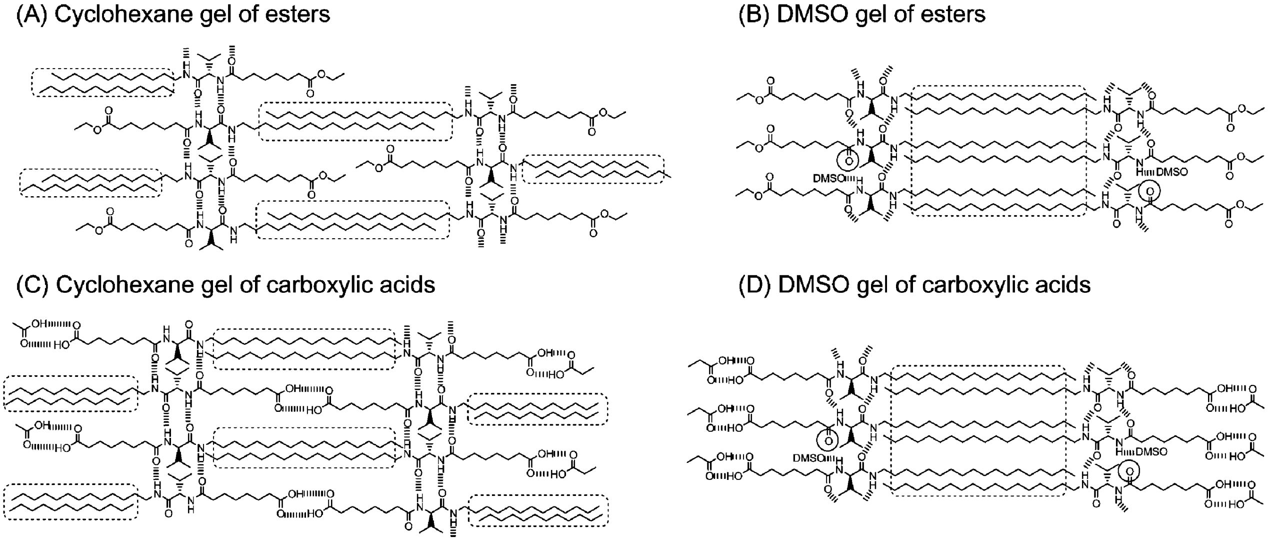

Scheme 2 Tentative illustration of aggregation modes in non-polar and polar solvents.

formed by binding modes similar to those of the ester-type gelators (Scheme 2(C)). The ester and hydrogen bonded carboxy groups are situated in aggregates thickly packed by alkyl groups (hydrophobic field), particularly, the suberic acid (C_6) derivative (**1a** and **1b**). Such a hydrophobic field brings about a strong hydrogen-bonding interaction in the carboxy dimer; therefore, the IR peak of the carboxy group shifts to a lower wavelength. In contrast, the ester groups of the succinic acid (C_2) derivatives approach the hydrogen bonding area of the amide groups (hydrophilic field).

On the other hand, the aggregation mode in the DMSO gel is different from that in the cyclohexane gel. In a polar solvent (DMSO), the hydrophobic domain is constructed by aggregation of the alkyl side chains through a van der Waals interaction, and most hydrogen-bonded DMSO molecules are removed from the domain to the bulk.[10] A hydrogen-bonding interaction between the amide groups simultaneously occurs. However, some DMSO molecules keep undergoing hydrogen bonding and the free C=O groups (amide) remain uninvolved (circles in Scheme 2(B) and (D)). The ester and hydrogen bonded carboxy groups could be easily exposed to the bulk solution. Therefore, the hydrogen-bonding interaction of the carboxy dimer in the DMSO gel is weaker than that of the cyclohexane gel, as supported by the IR results.

As demonstrated in Fig. 1, the microstructures of the organogels are nanofibers, which are formed by the aggregates shown in Scheme 2. However, the influence of the molecular packing on the formation of nanofibers is hardly observed in Fig. 1. It is likely that the balance of van der Waals and hydrogen bonding interactions changed by the hydrophilicity–hydrophobicity balance of a gelator molecule may play an important role in their growth into nanofibers.

Selective organogelation from oil/water

The selective gelation of oil from an oil/water or of water from an oil/water mixture is very important for the dissolution of an oil spill.[3g,11] The ester- and carboxy-type organogelators are suitable for selective gelation of an oil from water/oil mixtures due to their insolubility in water and good organogelation abilities for many oils. We investigated the selective gelation of a discrete volume of oil by **1b** when it is present in a two-phase system. Fig. 4 shows a typical procedure for the selective gelation in an oil/water mixed solution using **1b**. Water (0.9 mL) and a salad oil (0.1 mL) were placed in a sample tube and then **1b** (2 mg) was added to the two-phase solution. **1b** was solubilized either by heating or by the addition of an ethanol solution of **1b** to the oil layer. After dissolution, a salad oil gel is formed in the water pool (Fig. 4(b)), and then the organogel was separated from water by tweezing out or filtration (Fig. 4(c)). The same observation is also seen in other oils and fuels and when using other organogelators.

Conclusions

We revealed the synthesis of novel organogelators based on L-valine and L-isoleucine derivatives with various terminal groups and their organogelation properties. The ester-type compounds functioned as powerful organogelators that could form organogels in many organic solvents and oils at relatively low concentrations. The organogelation abilities decreased with the increasing hydrophilicity of the gelator molecules. It was found that the aggregation modes of the gelator molecules in a non-polar solvent (cyclohexane) were different from those

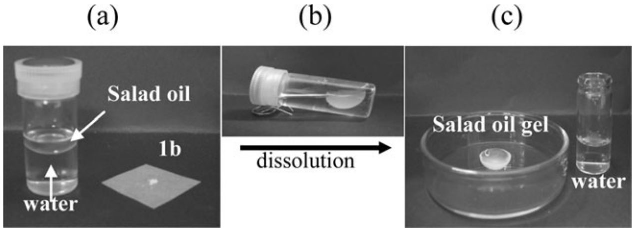

Fig. 4 Typical procedure for selective gelation.

in a polar solvent (DMSO). In addition, these gelators can selectively gel an oil from oil/water mixtures.

Experimental

Materials

L-Valylaminooctadecane and L-isoleucylaminooctadecane were prepared according to the literature.[7] The suberoyl chloride monomethyl ester was synthesized by the reaction of the corresponding acid in thionyl chloride and purified by distillation just before use. The other chemicals were of the highest commercially available grade and used without further purification. All solvents used in the syntheses were purified, dried, or freshly distilled as required.

General synthetic procedure for ester compounds 1, 4 and 7. To a dry THF solution of L-amino acid octadecylamine (20 mmol) and NEt_3 (10 mL), a freshly distilled acid chloride monoalkyl ester was slowly added at 0 °C with stirring and then the reaction mixture was stirred at room temperature for 12 h. The resulting solution was hot filtered and the filtrate was evaporated to dryness. The products were obtained by recrystallization from methanol-ether.

1a: Yield: 98%. IR (KBr) ν/cm^{-1}: 3291 (νN–H), 1737 (νC═O), 1634 (νC═O), 1541 (δN–H); ^{1}H NMR (400 MHz, $CDCl_3$, TMS, 25 °C): δ 0.88 (t, J = 6.6 Hz, 3H; CH_3), 0.93–0.95 (m, 6H; CH(CH_3)$_2$), 1.25–1.35 (m, 34H; alkyl), 1.45–1.51 (m, 2H; NHCH$_2$CH_2), 1.61–1.63 (m, 4H; OCOCH$_2$CH_2, NHCOCH$_2$CH_2), 2.00–2.09 (m, 1H; (CH$_3$)$_2$CH), 2.21 (t, J = 7.5 Hz, 2H; CH_2CON), 2.29 (t, J = 7.6 Hz, 2H; CH_2CO$_2$CH$_3$), 3.10–3.17 (m, 2H; NHCH_2), 3.66 (s, 3H; OCH_3), 4.21 (t, J = 8.6 Hz, 1H; NHCHCO), 6.31 (d, J = 8.8 Hz, 1H; CONHCH), 6.34 (t, J = 5.6 Hz, 1H; CONHCH$_2$); elemental analysis: calc. (%) for $C_{32}H_{62}N_2O_4$ (538.85): C, 71.33; H, 11.60; N, 5.20; found: C, 71.39; H, 11.98; N, 5.21.

4a: Yield: 91%. IR (KBr) ν/cm^{-1}: 3290 (νN–H, amide), 1736 (νC═O, ester), 1635 (νC═O, amide I), 1543 (δN–H, amide II). ^{1}H NMR (400 MHz, $CDCl_3$, TMS, 25 °C): δ 0.88 (t, J = 7.0 Hz, 3H; CH_3), 0.92–0.95 (m, 6H, CH(CH_3)$_2$), 1.25–1.26 (m, 33H; alkyl), 1.47–1.51 (m, 2H; NHCH$_2$CH_2), 1.61–1.63 (m, 4H; NHCOCH$_2$CH_2,OCOCH$_2$CH_2), 2.14–2.22 (m, 1H, (CH$_3$)$_2$CH), 2.43–2.57 (m, 2H; CH_2CONH), 2.61–2.71 (t, J = 7.1 Hz, 2H; CH_2CO$_2$CH$_2$CH$_3$), 3.12–3.33 (m, 2H, NHCH_2), 4.18 (t, J = 8.8 Hz, 1H; NHCHCO), 6.42 (t, J = 5.6 Hz, 1H; CH$_2$NHCO) 7.3 (d, J = 9.1 Hz, 1H; CONHCH$_2$); elemental analysis: calc. (%) for $C_{31}H_{60}N_2O_4$ (524.81): C, 70.94; H, 11.52; N, 5.34; found: C, 71.27; H, 11.87; N, 5.36.

7a: Yield: 93%. IR (KBr) ν/cm^{-1}: 3289 (νN–H, amide), 1738 (νC═O, ester), 1637 (νC═O, amide I), 1545 (δN–H, amide II). ^{1}H NMR (400 MHz, $CDCl_3$, TMS, 25 °C): δ 0.88 (t, J = 7.0 Hz, 3H; CH_3), 0.92–0.95 (m, 6H; CH(CH_3)$_2$), 1.25–1.26 (m, 33H; alkyl), 1.47–1.51 (m, 2H; NHCH$_2$CH_2), 2.14–2.22 (m, 1H, (CH$_3$)$_2$CH), 2.43–2.57 (m, 2H; CH_2CON), 2.61–2.71 (t, J = 7.1 Hz, 2H; CH_2CO$_2$CH$_2$CH$_3$), 3.1–3.3 (m, 2H, NHCH_2), 4.12 (q, 2H; OCH_2), 4.21 (t, J = 8.6 Hz, 1H; NHCHCO), 6.17 (t, J = 5.3 Hz, 1H; CONHCH$_2$), 6.22 (d, J = 8.8 Hz, 1H; CHNHCO); elemental analysis: calc. (%) for $C_{29}H_{58}N_2O_4$ (496.76): C, 70.12; H, 11.36; N, 5.64; found: C, 70.56; H, 11.74; N, 5.66.

1b: Yield: 97%. IR (KBr) ν/cm^{-1}: 3291 (νN–H), 1735 (νC═O), 1634 (νC═O), 1541 (δN–H); ^{1}H NMR (400 MHz, $CDCl_3$, TMS, 25 °C): δ 0.86–0.92 (m, 9H; CH_3), 1.25–1.35 (m, 36H; alkyl), 1.45–1.65 (m, 6H; alkyl), 1.80–1.84 (m, 1H; (CH$_3$)(CH$_3$CH$_2$)CH), 2.20 (t, J = 7.6 Hz, 2H; CH_2CON), 2.29 (t, J = 7.6 Hz, 2H; CH_2CO$_2$CH$_3$), 3.12–3.33 (m, 2H; NHCH_2), 4.20 (t, J = 8.1 Hz, 1H; NHCHCO), 6.02 (t, J = 5.1 Hz, 1H; CONHCH$_2$), 6.15 (d, J = 8.8 Hz, 1H; CONHCH); elemental analysis: calc. (%) for $C_{33}H_{64}N_2O_4$ (552.87): C, 71.69; H, 11.67; N, 5.07; found: C, 71.73; H, 11.84; N, 5.08.

4b: Yield: 86%. IR (KBr) ν/cm^{-1}: 3290 (νN–H), 1736 (νC═O, ester), 1635 (νC═O, amide I), 1543 (δN–H, amide II); ^{1}H NMR (400 MHz, $CDCl_3$, TMS, 25 °C): δ 0.86–0.92 (m, 9H; CH_3), 1.25–1.35 (m, 35H; alkyl), 1.45–1.65 (m, 6H; alkyl), 1.80–1.84 (m, 1H; (CH$_3$)(CH$_3$CH$_2$)CH), 2.22 (t, J = 7.3 Hz, 2H; CH_2CONH), 2.29 (t, J = 7.1 Hz, 2H; CH_2CO$_2$CH$_2$), 3.12–3.33 (m, 2H, NHCH_2), 4.12 (q, 2H; OCH_2CH$_3$), 4.22 (t, J = 8.1 Hz, 1H; NHCHCO), 6.02 (d, J = 8.8 Hz, 1H; CH$_2$NHCO), 6.15 (t, J = 5.6 Hz, 1H; CONHCH$_2$); elemental analysis: calc. (%) for $C_{32}H_{62}N_2O_4$ (538.84): C, 71.33; H, 11.60; N, 5.20; found: C, 71.69; H, 11.99; N, 5.25.

7b: Yield: 90%. IR (KBr) ν/cm^{-1}: 3289 (νN–H, amide), 1737 (νC═O, ester), 1638 (νC═O, amide I), 1544 (δN–H, amide II). ^{1}H NMR (400 MHz, $CDCl_3$, TMS, 25 °C): δ 0.86–0.95 (m, 9H; CH_3), 1.25–1.35 (m, 35H; alkyl), 1.51–1.56 (m, 2H; NHCH$_2$CH_2), 1.91–2.00 (m, 1H; (CH$_3$)(CH$_3$CH$_2$)CH), 2.20 (t, J = 7.6 Hz, 2H; CH_2CON), 2.29 (t, J = 7.6 Hz, 2H; CH_2CO$_2$CH$_3$), 3.17–3.33 (m, 2H, NHCH_2), 4.18 (q, 2H; OCH_2CH$_3$), 4.22 (t, J = 7.13 Hz, 1H; NHCHCO), 7.58 (d, J = 8.8 Hz, 1H; CH$_2$NHCO); elemental analysis: calc. (%) for $C_{30}H_{58}N_2O_4$ (510.77): C, 70.54; H, 11.45; N, 5.48; found: C, 71.00; H, 11.76; N, 5.53.

General synthetic procedure for carboxylic acids 2, 5 and 8. The ester (10 mmol) was dissolved in THF (300 mL) and 4 M NaOH$_{aq}$ (5 mL) was then added. After heating the reaction mixture at 60 °C for 24 h, the resulting solution was evaporated to dryness. The solid was dissolved in water (600 mL) and then the aqueous solution was acidified by *conc.* HCl (pH ≈ 1). The white precipitate was filtered off, washed with water, and then dried. The product was obtained by recrystallization from MeOH–diethyl ether.

2a: Yield: 96%. IR (KBr) ν/cm^{-1}: 3287 (νN–H), 1710 (νC═O), 1635 (νC═O), 1545 (δN–H); ^{1}H NMR (400 MHz, $CDCl_3$, TMS, 25 °C): δ 0.88 (t, J = 6.6 Hz, 3H; CH_3), 0.92–0.95 (m, 6H; CH(CH_3)$_2$), 1.25–1.27 (m, 34H; alkyl), 1.47–1.51 (m, 2H; NHCH$_2$CH_2), 1.59–1.68 (m, 4H; OCOCH$_2$CH_2, NHCOCH$_2$CH_2), 1.99–2.06 (m, 1H; (CH$_3$)$_2$CH), 2.22 (t, J = 7.6 Hz, 2H; CH_2CON), 2.33 (t, J = 7.1 Hz, 2H; CH_2CO$_2$H), 3.11–3.35 (m, 2H; NHCH_2), 4.18 (t, J = 8.6 Hz, 1H; NHCHCO), 6.44 (t, J = 5.6 Hz, 1H; CONHCH$_2$), 7.03 (d, J = 9.1 Hz, 1H; CONHCH); elemental analysis: calc. (%) for $C_{31}H_{60}N_2O_4$ (524.82): C, 70.94; H, 11.52; N, 5.34; found: C, 71.14; H, 11.84; N, 5.34.

5a: Yield: 94%. IR (KBr) ν/cm^{-1}: 3290 (νN–H, amide), 1711 (νC═O, COOH), 1635 (νC═O, amide I), 1543 (δN–H, amide II) ^{1}H NMR (400 MHz, $CDCl_3$, TMS, 25 °C): δ 0.88 (t, *J* = 6.6 Hz, 3H; CH_3), 0.92–0.95 (m, 6H, $CH(CH_3)_2$), 1.25–1.26 (m, 32H; alkyl), 1.49–1.70 (m, 6H; alkyl), 1.99–2.06 (m, 1H, $(CH_3)_2CH$), 2.22 (t, *J* = 7.6 Hz, 2H; CH_2CONH), 2.33 (t, *J* = 7.1 Hz, 2H; CH_2CO_2H), 3.12–3.33 (m, 2H, $NHCH_2$), 4.18 (t, *J* = 8.8 Hz, 1H; NHC*H*CO), 6.42 (t, *J* = 5.6 Hz, 1H; CH_2N*H*CO), 7.3 (d, *J* = 9.1 Hz, 1H; CON*H*CH_2); elemental analysis: calc. (%) for $C_{29}H_{58}N_2O_4$ (496.76): C, 70.12; H, 11.36; N, 5.64; found: C, 70.49; H, 11.99; N, 5.69.

8a: Yield: 93%. IR (KBr) ν/cm^{-1}: 3289 (νN–H, amide), 1718 (νC=O, COOH), 1638 (νC=O, amide I), 1544 (δN–H, amide II). ^{1}H NMR (400 MHz, $CDCl_3$, TMS, 25 °C): δ 0.88 (t, *J* = 7.1 Hz, 3H; CH_3), 0.92–0.95 (m, 6H, $CH(CH_3)_2$), 1.25–1.26 (m, 32H; alkyl), 1.47–1.51 (m, 2H; $NHCH_2CH_2$), 1.62–1.70 (m, 4H; $NHCOCH_2$, $OCOCH_2$), 1.99–2.10 (m, 1H, $(CH_3)_2CH$), 2.23 (t, *J* = 7.0 Hz, 2H; CH_2CON), 2.31 (t, *J* = 7.3 Hz, 2H; $CH_2CO_2CH_3$), 3.13–3.33 (m, 2H, $NHCH_2$), 4.18 (t, *J* = 8.6 Hz, 1H; NHC*H*CO), 5.18 (t, *J* = 5.6 Hz, 1H; CH_2N*H*CO), 7.0 (d, *J* = 8.6 Hz, 1H; CON*H*CH_2); elemental analysis: calc. (%) for $C_{27}H_{52}N_2O_4$ (468.71): C, 69.19; H, 11.18; N, 5.98; found: C, 69.88; H, 11.66; N, 6.01.

2b: Yield: 95%. IR (KBr) ν/cm^{-1}: 3289 (νN–H), 1710 (νC=O), 1635 (νC=O), 1543 (δN–H); ^{1}H NMR (400 MHz, $CDCl_3$, TMS, 25 °C): δ 0.86–0.90 (m, 9H; CH_3), 1.25–1.34 (m, 34H; alkyl), 1.475–1.51 (m, 2H; $CONHCH_2CH_2$), 1.58–1.67 (m, 4H; $NHCOCH_2CH_2$, $OCOCH_2CH_2$), 1.78–1.83 (m, 1H; $(CH_3)_2CH$), 2.20 (t, *J* = 6.6 Hz, 2H; CH_2CON), 2.33 (t, *J* = 6.8 Hz, 2H; $CH_2CO_2CH_3$), 3.12–3.33 (m, 2H; $NHCH_2$), 4.22 (t, *J* = 8.81 Hz, 1H; NHC*H*CO), 6.43 (t, *J* = 5.6 Hz, 1H; CON*H*CH_2), 7.05 (d, *J* = 9.1 Hz, 1H; CON*H*CH); elemental analysis: calc. (%) for $C_{32}H_{62}N_2O_4$ (538.85): C, 71.33; H, 11.60; N, 5.20; found: C, 71.35; H, 11.98; N, 5.21.

5b: Yield: 92%. IR (KBr) ν/cm^{-1}: 3289 (νN–H, amide), 1708 (νC=O, COOH), 1635 (νC=O, amide I), 1544 (δN–H, amide II) ^{1}H NMR (400 MHz, $CDCl_3$, TMS, 25 °C): δ 0.86–0.90 (m, 9H; CH_3), 1.25–1.35 (m, 32H; alkyl), 1.48–1.51 (m, 2H; $CONHCH_2CH_2$), 1.58–1.68 (m, 4H; $NHCOCH_2CH_2$), 1.80–1.82 (m, 1H; $(CH_3)(CH_3CH_2)CH$), 2.26 (t, *J* = 7.3 Hz, 2H; CH_2CONH), 2.33 (t, *J* = 7.6 Hz, 2H; CH_2CO_2H), 3.1–3.34 (m, 2H, $NHCH_2$), 4.22 (t, *J* = 8.8 Hz, 1H; NHC*H*CO), 6.02 (t, *J* = 5.3 Hz, 1H; CON*H*CH_2), 6.15 (d, *J* = 9.12 Hz, 1H; CH_2N*H*CO); elemental analysis: calc. (%) for $C_{30}H_{58}N_2O_4$ (510.79): C, 70.54; H, 11.45; N, 5.48; found: C, 70.76; H, 11.81; N, 5.50.

8b: Yield: 95%. IR (KBr) ν/cm^{-1}: 3287 (νN–H, amide), 1719 (νC=O, COOH), 1637 (νC=O, amide I), 1544 (δN–H, amide II); ^{1}H NMR (400 MHz, $CDCl_3$, TMS, 25 °C): δ 0.86–0.90 (m, 9H; CH_3), 1.25–1.35 (m, 32H; alkyl), 1.48–1.50 (m, 2H; $CONHCH_2CH_2$), 1.82 (m, 1H; $(CH_3)(CH_3CH_2)CH$), 2.20 (t, *J* = 6.6 Hz, 2H; CH_2CON), 2.33 (t, *J* = 6.8 Hz, 2H; $CH_2CO_2CH_3$), 3.12–3.33 (m, 2H, $NHCH_2$), 4.22 (t, *J* = 8.8 Hz, 1H; NHC*H*CO), 6.15 (t, *J* = 5.6 Hz, 1H; CON*H*CH_2), 7.55 (d, *J* = 8.6 Hz, 1H; CH_2N*H*CO); elemental analysis: calc. (%) for $C_{28}H_{54}N_2O_4$ (482.74): C, 69.66; H, 11.27; N, 5.80; found: C, 70.21; H, 11.68; N, 5.85.

General synthetic procedure for Na salts 3, 6 and 9. The carboxylic acid (10 mmol) was dissolved in MeOH (200 mL) and then 1 M $NaOH_{aq}$ (10 mL) was added. After stirring at room temperature for 20 min, the resulting solution was evaporated to dryness. The product was obtained by recrystallization from MeOH–diethyl ether.

3a: Yield: 99%. IR (KBr) ν/cm^{-1}: 3287 (νN–H), 1636 (νC=O), 1562 (δN–H); ^{1}H NMR (400 MHz, MeOH, TMS, 25 °C): δ 0.87–0.95 (m, 9H, CH_3, $CH(CH_3)_2$), 1.16–1.37 (m, 34H; alkyl), 1.48–1.51 (m, 2H; $NHCH_2CH_2$), 1.60–1.62 (m, 4H; $NHCOCH_2CH_2$, $OCOCH_2CH_2$), 1.99–2.06 (m, 1H, $(CH_3)_2CH$), 2.15 (t, *J* = 7.8 Hz 2H; CH_2CON), 2.2–2.3 (m, 2H; $CH_2CO_2CH_3$), 3.10–3.24 (m, 2H, $NHCH_2$), 4.08 (m, 1H; NHC*H*CO); elemental analysis: calc. (%) for $C_{31}H_{59}N_2O_4Na$ (546.80): C, 68.09; H, 10.88; N, 5.12; found: C, 68.21; H, 11.04; N, 5.12.

6a: Yield: 95%. IR (KBr) ν/cm^{-1}: 3289 (νN–H, amide), 1636 (νC=O, amide I), 1559 (δN–H, amide II). ^{1}H NMR (400 MHz, MeOH, TMS, 25 °C): δ 0.88 (t, *J* = 6.6 Hz 3H; CH_3), 0.92–0.95 (m, 6H; $CH(CH_3)_2$), 1.24–1.28 (m, 30H; alkyl), 1.48–1.51 (m, 2H; $NHCH_2CH_2$), 1.61–1.64 (m, 4H; $NHCOCH_2CH_2$,$OCOCH_2CH_2$), 1.99–2.07 (m, 1H, $(CH_3)_2CH$), 2.18 (t, *J* = 7.8 Hz, 2H; CH_2CON), 2.25–2.36 (m, 2H; $CH_2CO_2CH_3$), 3.11–3.22 (m, 2H, $NHCH_2$), 4.08 (d, *J* = 7.6 Hz, 1H; NHC*H*CO); elemental analysis: calc. (%) for $C_{29}H_{55}N_2NaO_4$ (518.74): C, 67.14; H, 10.69; N, 5.40; found: C, 67.69; H, 11.00; N, 5.44.

9a: Yield: 96%. IR (KBr) ν/cm^{-1}: 3289 (νN–H, amide), 1635 (νC=O, amide I), 1558 (δN–H, amide II). ^{1}H NMR (400 MHz, MeOH, TMS, 25 °C): δ 0.878–0.935 (m, 9H, CH_3, $CH(CH_3)_2$), 1.28 (m, 32H; alkyl), 1.48–1.51 (m, 2H; $NHCH_2CH_2$), 1.88–1.95 (m, 1H, $(CH_3)_2CH$), 2.41–2.54 (m, 4H; $NHCOCH_2$, $OCOCH_2$), 3.10–3.24 (m, 2H, $NHCH_2$), 4.17 (d, 6.56, 1H; NHC*H*CO); elemental analysis: calc. (%) for $C_{27}H_{51}N_2NaO_4$ (490.69): C, 66.09; H, 10.48; N, 5.71; found: C, 66.71; H, 10.88; N, 5.77.

3b: IR (KBr) ν/cm^{-1}: 3289 (νN–H), 1635 (νC=O), 1560 (δN–H); ^{1}H NMR (400 MHz, MeOH, TMS, 25 °C): δ 0.88–0.91 (m, 9H; CH_3), 1.21–1.28 (m, 36H; alkyl), 1.49–1.51 (m, 2H; $CONHCH_2CH_2$), 1.59–1.62 (m, 4H; $NHCOCH_2CH_2$), 1.80–1.85 (m, 1H; $(CH_3)(CH_3CH_2)CH$), 2.17–2.19 (m, 2H; CH_2CONH), 2.21–2.27 (m, 2H; CH_2CO_2H), 3.11–3.22 (m, 2H, $NHCH_2$), 4.13 (d, 1H; NHC*H*CO); elemental analysis: calc. (%) for $C_{32}H_{61}N_2O_4Na$ (560.83): C, 68.53; H, 10.96; N, 5.00; found: C, 68.71; H, 11.11; N, 5.01.

6b: Yield: 98%. IR (KBr) ν/cm^{-1}: 3289 (νN–H, amide), 1635 (νC=O, amide I), 1559 (δN–H, amide II) ^{1}H NMR (400 MHz, MeOH, TMS, 25 °C): δ 0.88–0.92 (m, 9H; CH_3), 1.21–1.28 (m, 32H; alkyl), 1.48–1.51 (m, 2H; $CONHCH_2CH_2$), 1.63–1.64 (m, 4H; $NHCOCH_2CH_2$), 1.80–1.85 (m, 1H; $(CH_3)(CH_3CH_2)CH$), 2.17–2.19 (m, 2H; CH_2CONH), 2.25–2.27 (m, 2H; CH_2CO_2H), 3.08–3.24 (m, 2H, $NHCH_2$), 4.14 (m, 1H; NHC*H*CO); elemental analysis: calc. (%) for $C_{30}H_{57}N_2NaO_4$ (532.77): C, 67.63; H, 10.78; N, 5.26; found: C, 67.88; H, 11.03; N, 5.30.

9b: Yield: 99%. IR (KBr) ν/cm^{-1}: 3289 (νN–H, amide), 1708 (νC=O, COOH), 1635 (νC=O, amide I), 1544 (δN–H, amide II). ^{1}H NMR (400 MHz, $CDCl_3$, TMS, 25 °C): δ 0.88–0.93 (m, 9H; CH_3), 1.21–1.28 (m, 32H; alkyl), 1.46–1.52 (m, 2H; $CONHCH_2CH_2$), 1.63–1.64 (m, 4H; $NHCOCH_2CH_2$), 1.87–1.94 (m, 1H; $(CH_3)(CH_3CH_2)CH$), 2.17–2.19 (m, 2H; CH_2CONH), 2.25–2.27 (m, 2H; CH_2CO_2H), 3.12–3.21

(m, 2H, NHC*H*$_2$), 4.17 (d, *J* = 6.3 Hz, 1H; NHC*H*CO); elemental analysis: calc. (%) for $C_{28}H_{53}N_2NaO_4$ (504.72): C, 66.63; H, 10.58; N, 5.55; found: C, 67.00; H, 10.91; N, 5.58.

General methods

Measurements

The elemental analyses were performed using a Perkin–Elmer series II CHNS/O analyzer 2400. The FT-IR spectra were recorded by a JASCO FS-420 spectrometer. The field emission scanning electron micrograph (FE-SEM) observations were carried out using a Hitachi S-5000 field emission scanning electron microscope. The ^{1}H NMR spectra were measured using a Bruker AVANCE 400 spectrometer with TMS as the standard.

Gelation test

A mixture of a weighed gelator in water (1 mL) in a sealed test tube (15 mm in diameter) was heated until a clear solution appeared. After allowing the solutions to stand at 25 °C for 6 h, the state of the solution was evaluated by the "test tube inversion" method.

FE-SEM

Samples were prepared as follows: the xerogels were prepared from the organogels and dried under vacuum for 24 h. The dried xerogels were covered with an approximately 10 nm thick Pt–Pd layer by sputtering.

FT-IR study

The FT-IR spectroscopy was performed in organic solvents operating at a 2 cm^{-1} resolution with 32 scans. A spectroscopic cell with CaF_2 windows and 50 μm spacers was used for the measurements.

Acknowledgements

This study was supported by a Grant-in-aid for the 21st Century COE program and a Grant-in-aid for Exploratory Research (No. 17655049) by the Ministry of Education, Culture, Sports, Science and Technology of Japan and by the Tokuyama Science Foundation.

References

1 (*a*) R. Langer, *Acc. Chem. Res.*, 2000, **33**, 94; (*b*) N. A. Peppas, Y. Huang, M. Tottes-Lugo, J. H. Ward and J. Zhang, *Ann. Rev. Biomed. Eng.*, 2000, **2**, 9; (*c*) K. Yong and D. J. Mooney, *Chem. Rev.*, 2001, **101**, 1869.
2 (*a*) F. Fages, F. Vogtle and M. Zinic, *Top. Curr. Chem.*, 2005, **256**, 77; (*b*) *Molecular Gels: Materials with Self-assembled Fibrillar Networks*, ed. P. Terech and R. G. Weiss, Springer, Dordrecht, 2006.
3 (*a*) P. Terech and R. G. Weiss, *Chem. Rev.*, 1997, **97**, 3313; (*b*) J. H. van Esch and B. L. Feringa, *Angew. Chem., Int. Ed.*, 2000, **39**, 2263; (*c*) D. J. Abdallah and R. G. Weiss, *Adv. Mater.*, 2000, **12**, 1237; (*d*) L. Estroff and A. D. Hamilton, *Chem. Rev.*, 2004, **104**, 1201; (*e*) M. de Loos, B. L. Feringa and J. H. van Esch, *Eur. J. Org. Chem.*, 2005, 3615; (*f*) N. M. Sangeetha and U. Maitra, *Chem. Soc. Rev.*, 2005, **34**, 821.
4 (*a*) H. Kobayashi, A. Friggeri, K. Koumoto, M. Amaike, S. Shinkai and D. N. Reinhoudt, *Org. Lett.*, 2002, **4**, 1423; (*b*) A. Heeres, C. van der Pol, M. Stuart, A. Friggeri, B. L. Feringa and J. van Esch, *J. Am. Chem. Soc.*, 2003, **125**, 14252; (*c*) S. Kiyonaka, K. Sada, I. Yoshimura, S. Shinkai, N. Kato and I. Hamachi, *Nat. Mater.*, 2004, **3**, 58; (*d*) S. Bhuniya, S. M. Park and B. H. Kim, *Org. Lett.*, 2005, **7**, 1741; (*e*) R. Karinaga, Y. Jeong, S. Shinkai, J. Kaneko and K. Sakurai, *Langmuir*, 2005, **21**, 9398; (*f*) A. Srivastave, S. Ghorai, A. Bhattacharjya and S. Bhattacharya, *J. Org. Chem.*, 2005, **70**, 6574; (*g*) K. Köhler, A. Meister, G. Förster, B. Dobner, S. Drescher, F. Ziethe, W. Richer, F. Steiniger, M. Drechsler, G. Hause and A. Blume, *Soft Matter*, 2006, **2**, 77; (*h*) Z. Yang, G. Liang and B. Xu, *Chem. Commun.*, 2006, 738.
5 M. Suzuki, Y. Sakakibara, S. Kobayashi, M. Kimura, H. Shirai and K. Hanabusa, *Polym. J. (Tokyo, Jpn.)*, 2002, **34**, 474.
6 (*a*) K. Murata, M. Aoki, T. Suzuki, T. Harada, H. Kawabata, T. Komori, F. Ohseto, K. Ueda and S. Shinkai, *J. Am. Chem. Soc.*, 1994, **116**, 6664; (*b*) J. H. Jung, Y. Ono and S. Shinkai, *Chem.–Eur. J.*, 2000, **6**, 4552; (*c*) S. Kobayashi, N. Hamasaki, M. Suzuki, M. Kimura, H. Shirai and K. Hanabusa, *J. Am. Chem. Soc.*, 2002, **124**, 6550; (*d*) J. D. Hartgerinl, E. Beniash and S. I. Stupp, *Science*, 2001, **294**, 1684; (*e*) Y. Yang, M. Suzuki, M. Kimura, H. Shirai and K. Hanabusa, *Chem. Commun.*, 2004, 1332; (*f*) Y. Yang, M. Suzuki, H. Shirai, A. Kurose and K. Hanabusa, *Chem. Commun.*, 2005, 2032; (*g*) Y. Zhou, O. Ji, M. Masuda, S. Kamiya and T. Shimizu, *Chem. Mater.*, 2006, **18**, 403; (*h*) M. Suzuki, Y. Nakajima, T. Sato, H. Shirai and K. Hanabusa, *Chem. Commun.*, 2006 377.
7 K. Hanabusa, R. Tanaka, M. Suzuki, M. Kimura and H. Shirai, *Adv. Mater.*, 1997, **9**, 1095.
8 If the ester group has a hydrogen bonding interaction, the IR peak should shift to a lower wavelength.
9 X. Luo, B. Liu and Y. Liang, *Chem. Commun.*, 2001, 1556.
10 In DMSO, the N–H undergoes a hydrogen bonding with DMSO [$(CH_3)_2S{=}O\cdots H{-}N$] and the C=O groups are free.
11 S. Bhattacharya and Y. Krishnan-Ghosh, *Chem. Commun.*, 2001, 185.